Published OnlineFirst November 19, 2015; DOI: 10.1158/1535-7163.MCT-15-0207

Large Molecule Therapeutics

Molecular Cancer Therapeutics

Nanoconjugation of PSMA-Targeting Ligands Enhances Perinuclear Localization and Improves Efficacy of Delivered Alpha-Particle Emitters against Tumor Endothelial Analogues

Charles Zhu[1], Amey Bandekar[2], Michelle Sempkowski[1], Sangeeta Ray Banerjee[3], Martin G. Pomper[3], Frank Bruchertseifer[4], Alfred Morgenstern[4], and Stavroula Sofou[1,2]

Abstract

This study aims to evaluate the effect on killing efficacy of the intracellular trafficking patterns of α-particle emitters by using different radionuclide carriers in the setting of targeted antivascular α-radiotherapy. Nanocarriers (lipid vesicles) targeted to the prostate-specific membrane antigen (PSMA), which is unique to human neovasculature for a variety of solid tumors, were loaded with the α-particle generator actinium-225 and were compared with a PSMA-targeted radiolabeled antibody. Actinium-225 emits a total of four α-particles per decay, providing highly lethal and localized irradiation of targeted cells with minimal exposure to surrounding healthy tissues. Lipid vesicles were derivatized with two types of PSMA-targeting ligands: a fully human PSMA antibody (mAb) and a urea-based, low-molecular-weight agent. Target selectivity and extent of internalization were evaluated on monolayers of human endothelial cells (HUVEC) induced to express PSMA in static incubation conditions and in a flow field. Both types of radiolabeled PSMA-targeted vesicles exhibit similar killing efficacy, which is greater than the efficacy of the radiolabeled control mAb when compared on the basis of delivered radioactivity per cell. Fluorescence confocal microscopy demonstrates that targeted vesicles localize closer to the nucleus, unlike antibodies which localize near the plasma membrane. In addition, targeted vesicles cause larger numbers of dsDNAs per nucleus of treated cells compared with the radiolabeled mAb. These findings demonstrate that radionuclide carriers, such as PSMA-targeted lipid-nanocarriers, which localize close to the nucleus, increase the probability of α-particle trajectories crossing the nuclei, and, therefore, enhance the killing efficacy of α-particle emitters. *Mol Cancer Ther; 15(1); 106–13. ©2015 AACR.*

Introduction

The importance of antivascular therapy in the adjuvant treatment of cancer is well recognized (1). Critical prerequisites in this scenario, however, include the selective targeting of the tumor vasculature and the targeted delivery of highly lethal therapeutics. Among numerous antivascular agents developed and studied (1–3), α-particle emitters are identified for their exceptional suitability (3, 4). This is due to the high linear energy transfer (LET; of the order of 80 keV/μm) and short range (50–100 μm) of α-particles resulting in highly lethal and localized irradiation of the tumor vasculature. To increase the killing efficacy of delivered radioactivity further, although not traditionally considered for α-particle emitters (5), different radionuclide carriers could be evaluated to explore potentially favorable spatiotemporal intracellular distributions (intracellular trafficking) of the α-emitters which could increase the probability of nuclear hits.

The design of preclinical studies, which aim to evaluate experimental neovasculature-targeting constructs, faces at least two major technical limitations. Human tumor endothelial cells expressing human antigens of targeting interest are practically still not available in culture (6), and in animal models the neovasculature and its antigens are of host-origin. To emulate tumor endothelium analogues *in vitro*, we utilize a parallel-plate flow chamber with a controlled flow field containing the targeted therapeutics and with walls coated with monolayers of model human endothelial cells (HUVEC) induced to express the prostate-specific membrane antigen (PSMA). PSMA is a homodimeric type II integral membrane glycoprotein, is selectively found in the neovasculature of patients with several PSMA-negative tumors, and is absent in the healthy endothelium (7, 8).

In this study, we hypothesize that the patterns of intracellular trafficking of delivered α-particle emitters may significantly affect the efficacy of the delivered radioactivity. In order to explore this hypothesis, we designed lipid-based nanocarriers (lipid vesicles) loaded with the α-particle generator Actinium-225 (^{225}Ac) and labeled the vesicles with two different types of PSMA-targeting ligands, which appear to target similar epitopes of PSMA: a fully human PSMA antibody (mAb), and a urea-based low-molecular-weight agent (9). The therapeutic generator ^{225}Ac emits a total of

[1]Department of Biomedical Engineering, Rutgers University, Piscataway, New Jersey. [2]Department of Chemical and Biochemical Engineering, Rutgers University, Piscataway, New Jersey. [3]Russell H. Morgan Department of Radiology and Radiological Science, Johns Hopkins Medical School, Baltimore, Maryland. [4]European Commission, Joint Research Centre, Institute for Transuranium Elements, Karlsruhe, Germany.

Note: Supplementary data for this article are available at Molecular Cancer Therapeutics Online (http://mct.aacrjournals.org/).

C. Zhu and A. Bandekar contributed equally to this article.

Corresponding Author: Stavroula Sofou, Rutgers University, 599 Taylor Road, Piscataway, NJ 08854. Phone: 848-445-6568; Fax: 732-445-3753; E-mail: ss1763@rci.rutgers.edu

doi: 10.1158/1535-7163.MCT-15-0207

Published OnlineFirst November 19, 2015; DOI: 10.1158/1535-7163.MCT-15-0207

four α-particles per decay (10). We evaluate both vesicle constructs and compare with the radiolabeled antibody in terms of targeting selectivity and killing efficacy, which are then compared with the intracellular trafficking patterns and any resulting dsDNA for all constructs.

Materials and Methods

Materials

The lipids 2-dihenarachidoyl-sn-glycero-3-phosphocholine (21PC), 1,2-distearoyl-sn-glycero-3-phosphoethanolamine-N-[Methoxy(Polyethylene glycol)-2000] (Ammonium Salt; DSPE-PEG), 1,2-distearoyl-sn-glycero-3-phosphoethanolamine-N-[PDP (Polyethylene Glycol) 2000] (Ammonium Salt; PDP-PEG-lipid), 1,2-dipalmitoyl-sn-glycero-3-phosphoethanolamine-N-(LissamineRhodamine B Sulfonyl) (Ammonium Salt; DPPE-Rhodamine) were purchased from Avanti Polar Lipids and were used without further purification (all lipids at purity > 99%). 1,4,7,10-tetraazacyclododecane-1,4,7,10-tetraacetic acid (DOTA) and p-SCN-Bn-DOTA (DOTA-SCN) were purchased from Macrocyclics. Cholesterol (Chol), PBS, Sephadex G-50, Sepharose 4B, sodium carbonate, tetramethylammonium acetate (TMAA), sodium chloride (NaCl), glycine, sucrose, diethylenetriaminepentaacetic acid (DTPA), calcium ionophore A23187, dithiothreitol (DTT), 4-(2-hydroxyethyl)-1-piperazineethanesulfonic acid (HEPES), Endothelial Cell Growth Supplement (ECGS), heparin sodium salt, and *N*,*N*-dimethylformamide (DMF) were purchased from Sigma-Aldrich Chemical. Ethylenediaminetetraaceticd acid, disodium salt Dihydrate (EDTA) was purchased from Fisher Scientific. FBS was purchased from Omega Scientific. CellTiter 96 Non-Radioactive cell proliferation assay (MTT) was purchased from Promega Corporation. Matrigel was purchased from BD Biosciences. 10DG and PD10 desalting columns were obtained from BioRad. For isotype control antibody, a human IgG1K (catalog number 0151K-01) was purchased from Southern Biotech. Actinium-225 (^{225}Ac, actinium chloride) was provided by the Institute for Transuranium Elements.

For the synthesis of lysine-glutamate urea conjugated to the free polymer chain(s) of 1,2-distearoyl-sn-glycero-3-phosphoethanolamine-N- [amino(polyethylene glycol)-2000] (DSPE-PEG(2000)), a solution of N-hydroxysuccinimide ester of suberate lysine-glutamate urea (ref. 11; 5 mg, 8.98 μmol, in 500 μL DMF) was added to DSPE-PEG(2000) (10 mg, 3.6 μmol in 900 μL DMF) followed by N,N-diisopropylethylamine (DIEA; 3 μL, 18 μmol). The reaction mixture was stirred at room temperature for 2 hours, and was then concentrated under reduced pressure at approximately 40°C. The semi-solid residue thus obtained was washed with 5 × 1 mL 80/20 water/acetonitrile solution to remove unreacted lysine-glutamate urea. The colorless product was dried under high vacuum for 20 hours and was used for experiments. The synthesis yield was approximately 90% and with m/Z: 1594.5 [M+1]2+ by ElectroSpray Mass Spectrometry. The molecular structure of the functionalized lipid with a nonactive analogue (negative control) of the urea ligand is shown in Supplementary Fig. S1C. The targeting urea molecule is a small molecule (not a peptide), therefore, for the design of the negative control, a linker was attached to the lipid.

Lipid vesicle preparation and loading of constructs with ^{225}Ac

Vesicles composed of 21PC:Chol:DSPE-PEG:DPPE-Rhodamine at the mole ratio of 66.0:28.3:4.7:1.0 were formed using the thin film hydration method. All vesicles were labeled with 1 mole% of DPPE-Rhodamine lipid. For all targeted vesicles, either 0.5 mole% of the lysine-glutamate urea-based lipid (urea-lipid ref. 9) conjugate (resulting in a mole ratio of 65.7:28.2:4.7:0.9:0.5 21PC:chol:DSPE-PEG:DPPE-Rhodamine:lipid-urea) was included during the vesicle preparation step or the PSMA targeting antibody (Progenics Pharmaceuticals, Inc.) was conjugated on the PDP-modified free ends of PEG-chains using standard click-chemistry (12). Vesicles were suspended in HEPES buffer (20 mmol/L HEPES, 250 mmol/L sucrose at pH = 7.4) and were prepared to encapsulate citrate buffer (140 mmol/L citrate buffer with 5 mg/mL DOTA and 2.1 mg/mL ascorbic acid, pH 5.0). Vesicle size was measured using a Zetasizer NanoSeries (Malvern Instruments Ltd).

To load ^{225}Ac in vesicles, 1 mL (5 mmol/L total lipid) of vesicle suspension was incubated for 60 minutes at 80°C in a dry heating bath with 0.08 mL of a solution containing the following: 0.03 mL of ^{225}Actinium in 3 mmol/L HCl combined with 0.05 mL suspension of A23187 in an equimolar mixture of ethanol and water and at a final concentration in the vesicle suspension of 0.37 mg A23187/mL. After one hour of incubation, 0.05 mL of 10 mmol/L DTPA was added to the vesicle suspension to complex any unentrapped ^{225}Ac or ^{225}Ac adsorbed on the vesicle surface (12). Purification and determination of loading efficiency were performed using size exclusion chromatography with a 10-cm Sephadex G-50 column eluted with PBS (pH = 7.4, 300 mOsm) and by measuring radioactivity associated with the eluted vesicle suspension.

Antibody radiolabeling was performed using a two-step process which involved radiolabeling of a isothiocyanate-functionalized derivative of DOTA at 60°C in 2 mol/L tetramethylammonium acetate followed by labeling of antibodies with the radioactive chelate at lower temperature (13). The final eluted sample was evaluated for radiochemical purity and radiolabeling efficiency using ITLC.

Characterization of targeted constructs

Immunoreactivity of the urea-based ligand (11) and of the antibody (before and) after conjugation to vesicles was evaluated on the stably PSMA-positive LnCaP cell line in monolayers using antigens in excess of the ligands. The apparent-binding affinity K_D of targeted vesicles was evaluated on fixed, but not permeabilized, $PSMA^+$ HUVEC by measuring the cell-associated radioactivity on cells incubated with targeted ^{225}Ac-loaded vesicles using serial dilutions, and on cells incubated in addition with 50 times excess of targeted non-radiolabeled vesicles (14).

Cell lines and preparation of cell conditioned media

All cell lines (HUVEC and MDA-MB-231) were acquired from ATCC in 2013 and 2014, and were cultured in media suggested by ATCC supplemented with 10% FBS, 100 U/mL penicillin, and 100 μg/mL streptomycin in an incubator at 37°C and 5% CO_2. F12-K medium, used for HUVEC, was additionally supplemented with Heparin sodium salt (0.1 mg/mL) and ECGS (0.03 mg/mL). ATCC uses the following characterization tests: post-freeze viability, confirmation that cells are adherent, cell morphology, mycoplasma contamination, confirmation that cells are human in origin, and confirmation that cells do not contain pathogenic viruses. Cell conditioned media (CCM) were generated from the MDA-MB-231 breast cancer cell line (15).

Published OnlineFirst November 19, 2015; DOI: 10.1158/1535-7163.MCT-15-0207

Induction of PSMA expression on HUVEC cells

HUVEC cells were plated on Matrigel at a density of 10^6 cells per mL of CCM and were incubated in a humidified incubator at 37°C and 5% CO_2 for 18 hours according to a published method (15). Upon completion of incubation, PSMA expression was evaluated fluorometrically by immunofluorescence measured in a FACS Calibur flow cytometer and by Western blot analysis.

In particular, suspensions of fixed (with paraformaldehyde) HUVEC which previously had been carefully scraped and had been separated from Matrigel by centrifugation (277 × *g* for 5 minutes) were incubated for 60 minutes with a primary human anti-PSMA mouse monoclonal antibody (LifeSpan BioSciences, Inc.) followed by an additional 60-minute incubation with a FITC-labeled goat anti-mouse Fc secondary antibody (Jackson ImmunoResearch Laboratories). PSMA-positive LnCaP cells and PSMA-negative (not activated) HUVEC cells were also evaluated.

For Western blot analysis, cell lysate proteins were processed through SDS-PAGE under reducing conditions, followed by transfer onto nitrocellulose membrane. Membrane was blocked with 5% non-fat dry milk in TBST (20 mmol/L Tris, 150 mmol/L NaCl, 0.05% Tween-20) for 1 hour at room temperature, probed with primary mouse anti-PSMA antibody (ab19071, Abcam) in 0.5% milk in TBST for 1 hour at room temperature, and washed three times with TBST. The membrane was then probed with goat anti-mouse IgG-HRP conjugate (A24518, Life Technologies) for 1 hour at room temperature and then washed three times with TBST. Color was developed by adding HRP substrate (1706431, Bio-Rad) and incubating for 30 minutes.

Cell association of delivered radioactivity and cell viability studies

Binding of constructs under flow was determined using a rectangular parallel plate flow chamber (Glycotech). For $PSMA^+$ HUVEC, studies were initiated by introduction of ^{225}Ac-loaded constructs in CCM at a lipid concentration of 83.33 μmol/L and activity of 37 kBq/mL at a constant flow rate of 0.1 mL/minute using a PHD Ultra Syringe Pump (Harvard Apparatus) at 37°C and 5% CO_2. Parallel experiments were performed under static conditions. For studies on $PSMA^-$ HUVEC, cells were directly plated on fibronectin-covered slides

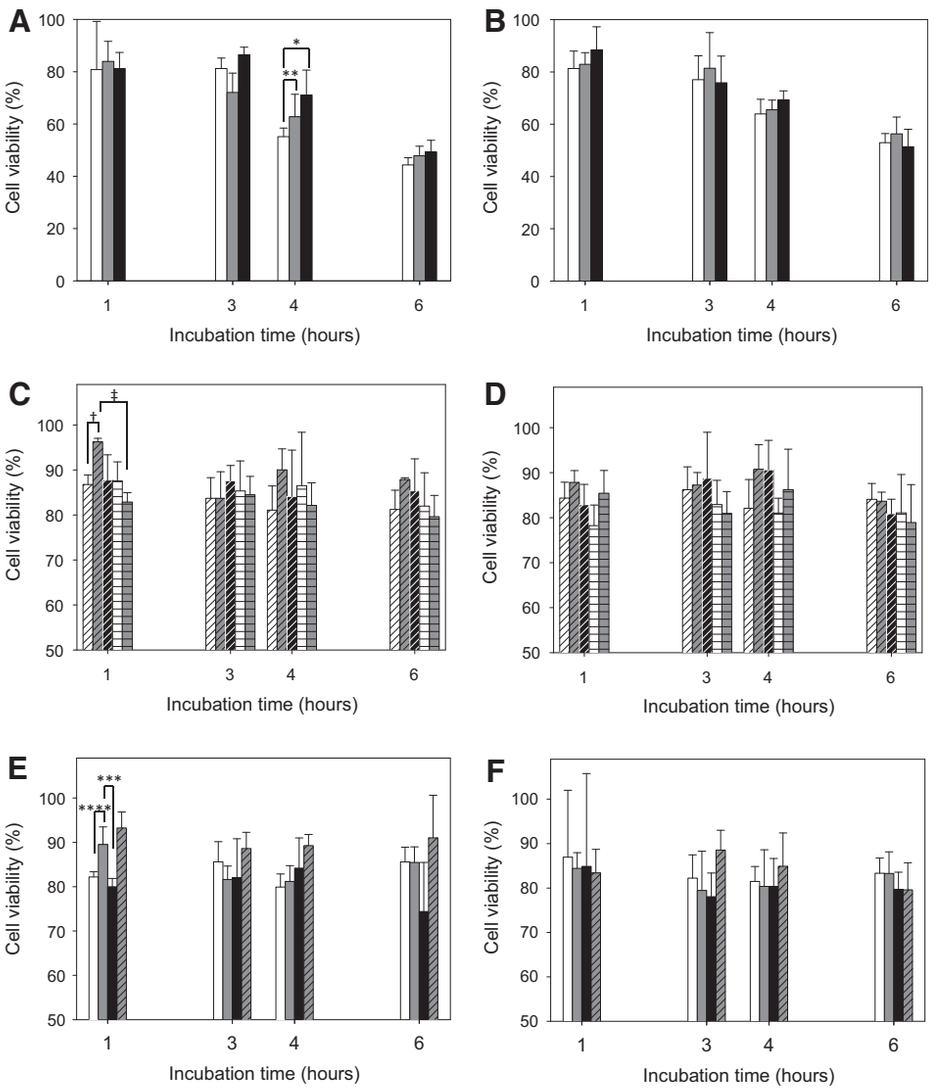

Figure 1.
Viability of PSMA-positive (A–D) and PSMA-negative HUVEC (E and F) in monolayers after treatment by various constructs loaded with ^{225}Ac for different incubation times in static incubation conditions (A, C, and E), and in the presence of a flow field (15 s^{-1} shear rate; B, D, and F). White bars, Ab-labeled vesicles; gray bars, urea-based labeled vesicles; black bars, radiolabeled Ab; white bars with tilted pattern, vesicles containing no targeting group loaded with ^{225}Ac; gray bars with tilted pattern, ^{225}Ac-DOTA chelate at activity levels corresponding to the values released from lipid vesicles; black bars with tilted pattern, nonradiolabeled antibody. White bars with horizontal pattern, ^{225}Ac-loaded vesicles labeled with an non-specific antibody; gray bars with horizontal pattern, ^{225}Ac-loaded vesicles labeled with an non-active urea analog. Viability evaluated after three doubling times. Error bars, SD of repeated measurements (2 and 3 independent preparations for antibodies and for vesicles, respectively, 2 measurements per preparation; *, $P = 0.044$; **, $P = 0.063$; †, $P = 0.039$; ‡, $P = 0.031$; ***, $P = 0.012$; ****, $P = 0.007$; all other cases $P > 0.12$).

Published OnlineFirst November 19, 2015; DOI: 10.1158/1535-7163.MCT-15-0207

in regular F12-K media as also were all constructs. At the end of incubation, cells were washed twice using ice cold PBS and were resuspended in F12-K media with 10% FBS, were counted using a hemocytometer, and were then used to determine (i) the cell associated radioactivity by counting the γ-emissions of Bismuth-213 upon reaching secular equilibrium; (ii) the extent of cell internalized radioactivity; and (iii) the viability of cells using the MTT assay. The extent of ^{225}Ac retention by all constructs was measured on a fraction of cell-exposed suspension using size exclusion chromatography.

Intracellular localization of constructs imaged by confocal microscopy

HUVECs were incubated under static conditions with nonradioactive, rhodamine-tagged vesicles or FITC-labeled antibody in the presence (see below) or absence of endocytosis inhibitors. After completion of incubation (6 hours), HUVECs were fixed with paraformaldehyde (4% in PBS for 10 minutes) before Hoechst 33342 staining, and then washed (3x) with PBS. Monolayers were imaged using a Leica TCS SP2 confocal laser scanning microscope under a 40× and an oil immersion 100× objective. For quantitative intracellular distributions of all constructs, a dilation protocol was applied. The fluorescence image of each cell nucleus was thresholded to yield a binary space that represented the boundaries of the nucleus. A circular morphologic structuring element was used to follow the edges of the thresholded nucleus image forming multiple concentric rings that expanded outward from the nucleus to the plasma membrane of the cell. The sum of pixel intensities within each ring was normalized to the sum of pixel intensities over the entire cell and graphed relative to the distance from the nucleus edge.

Characterization of cellular uptake mechanism

PSMA$^+$ HUVECs were incubated for 30 minutes with chlorpromazine (10 μg/mL) or with genistein (100 μg/mL) before incubation with fluorescently labeled constructs. Upon completion of incubation, cells were washed and evaluated for fluorescence uptake using flow cytometry. In presaturation experiments, cells were incubated for 60 minutes with 1,000× excess of free PSMA antibody (25 μg/mL) or the free lysine glutamate urea agent (0.1 μg/mL; ref. 16) before incubation with fluorescently labeled constructs.

Immunofluorescent staining of γ-H2AX foci

Phosphorylation of histone γ-H2AX was imaged by immunofluorescence using the same confocal microscope as above. The γ-H2AX foci were treated as biomarkers of dsDNA breaks induced by the emitted α-particles. Upon completion of incubation with radioactivity, cells were washed and fixed in 4% paraformaldehyde for 10 minutes at room temperature, and were permeabilized using 0.1% Triton X-100 in PBS. After permeabilizing for 5 minutes at room temperature, cells were stained for γ-H2AX using OxiSelect DNA Double Strand Break kit from CellBioLabs per kit instructions.

Statistical analysis

Results are reported as the arithmetic mean of n independent measurements ± the SD. The Student t test was used to calculate significant differences in killing efficacy between the various constructs. P values less than 0.01 are considered to be significant.

Results

Lipid vesicle characterization

The average vesicle size was 107 ± 5 nm ($n = 12$); PDI = 0.06 ± 0.04 ($n = 12$). Antibody conjugation resulted in 31 ± 9 antibodies per vesicle ($n = 4$), and the optimization studies on urea-based targeted vesicles indicated that a density of approximately 368 urea-based ligands per vesicle exhibit best uptake (Supplementary Fig. S1). The immunoreactivity of the radiolabeled antibody was 88.6 ± 0.8%. The apparent immunoreactivity of the antibody-labeled vesicles was 18.1 ± 1.5% ($n = 3$), and of the urea-labeled vesicles was 15.8 ± 1.6% ($n = 3$). Targeted vesicles exhibited limited association with PSMA-positive cells upon receptor blocking with the targeting antibody (0.1 ± 0.0% and 3.9 ± 3.7% for antibody- and urea-targeted vesicles, respectively).

The equilibrium binding affinity (K_D) was estimated from nonlinear regression curve fit analysis ($0.97 < R^2 < 1$) for the antibody-labeled vesicles (35.6 ± 1.5 μmol/L), the urea-based labeled vesicles (147 ± 9 μmol/L), and the radiolabeled antibody (22.9 ± 2.1 nmol/L; Supplementary Fig. S2A–S2C, respectively).

The average loading efficiency of ^{225}Ac in all targeted and nontargeted vesicles was 47.1 ± 16.6% ($n = 16$). In the presence of cells, vesicles retained 78.5 ± 3.6% ($n = 16$) of encapsulated radioactivity for the entire length of studies. The antibody radiolabeling efficiency was 3.4 ± 0.3% ($n = 2$). Antibody radiolabeling was stable (86.3 ± 2.3% of radioactivity retained, $n = 2$) for the length of the reported studies.

PSMA expression by HUVEC

HUVEC cells incubated with CCM on Matrigel expressed PSMA at significant levels (63 mean shift with respect to a shift of 3 for untreated cells, Supplementary Fig. S3A; and positive staining by Western blot analysis, Supplementary Fig. S3B) relative to the

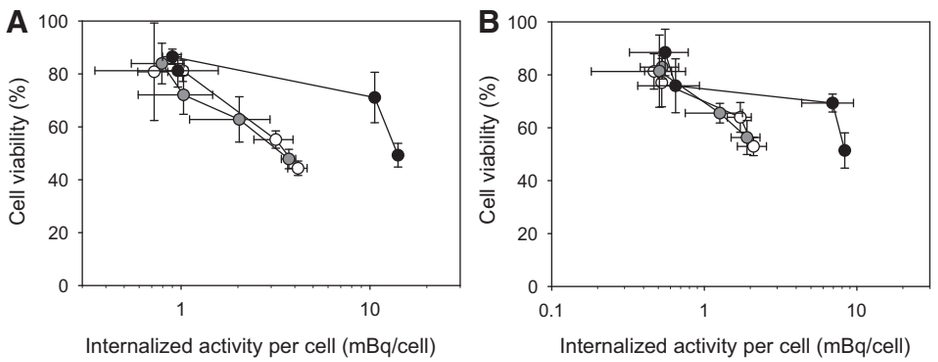

Figure 2.
Viability of PSMA-positive HUVEC as a function of delivered radioactivity per cell mediated by the Ab-targeted radiolabeled vesicles (white symbols), the urea-based targeted radiolabeled vesicles (gray symbols), and radiolabeled antibody (black symbols), in static incubation conditions (A), and in the presence of a flow field (B). Data replotted from Fig. 1 and Supplementary Table S2.

Published OnlineFirst November 19, 2015; DOI: 10.1158/1535-7163.MCT-15-0207

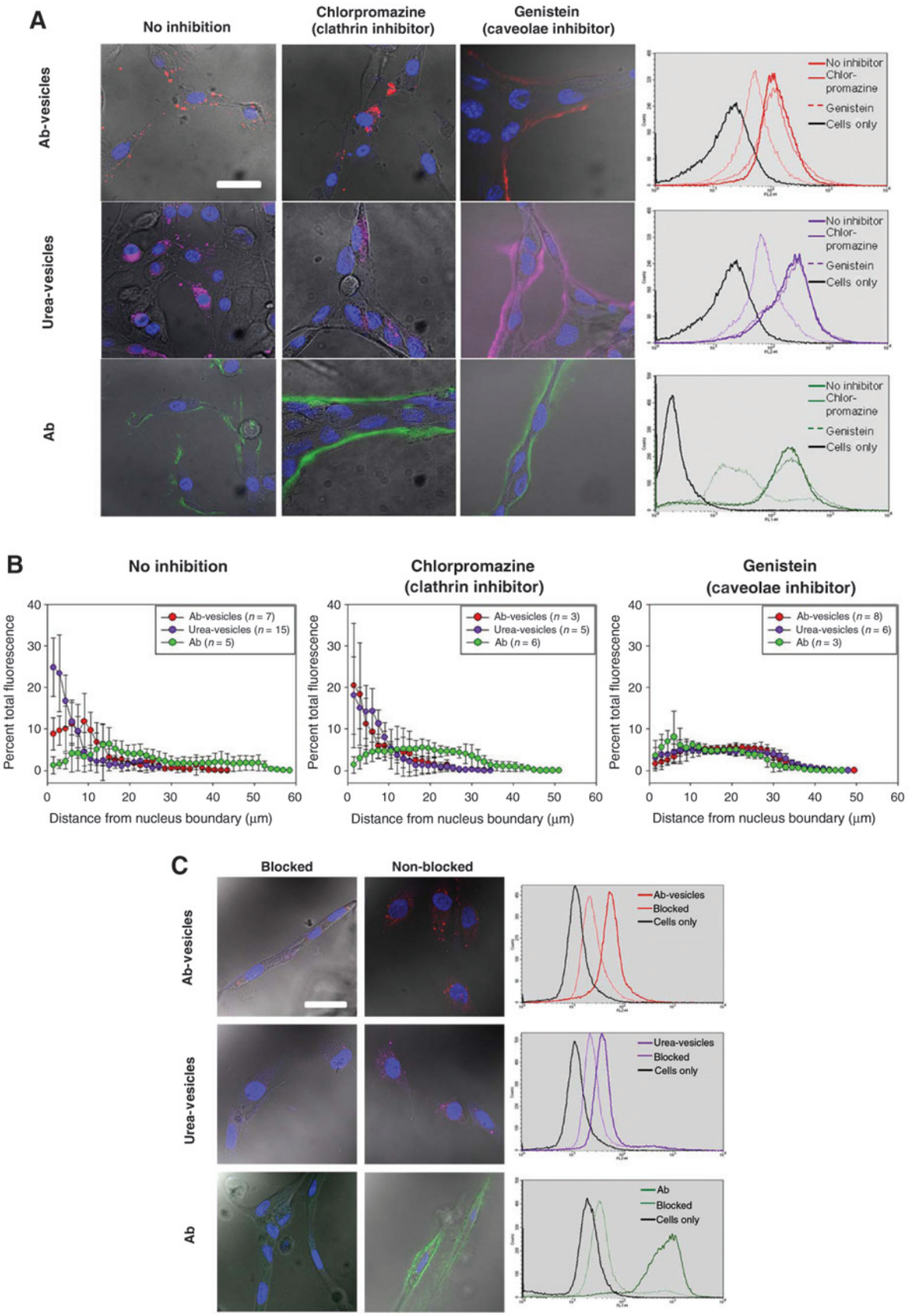

Published OnlineFirst November 19, 2015; DOI: 10.1158/1535-7163.MCT-15-0207

stably PSMA-positive cell line LnCaP (255 mean shift) corresponding to a reported 1.8×10^5 PSMA receptors per cell (17). Because removal of CCM, upon completion of the initial 18-hour incubation period, resulted in decrease of PSMA expression by HUVEC over time (Supplementary Fig. S4), all reported studies were performed in the presence of CCM to ensure stable PSMA expression. Finally, introduction of a flow field (at 15 s^{-1} shear rate) overlaying HUVEC decreased the PSMA expression in HUVEC by a factor of almost three relative to static culture conditions (Supplementary Table S1).

Killing efficacy and cell-associated radioactivity delivered by different constructs

Specific cell association of delivered radioactivity significantly increased with incubation time for all targeted constructs ($P < 0.01$) and depended on incubation conditions (static and under flow; Supplementary Table S2). Both types of targeted vesicles delivered comparable radioactivities per cell with similar extents of internalization. For comparison, the ^{225}Ac-labeled antibody delivered significantly greater levels of radioactivity per cell relative to targeted vesicles at the longer incubation times (4 and 6 hours; $P < 0.01$).

Across all targeted constructs loaded with ^{225}Ac, viabilities of PSMA-positive HUVEC exhibited significant decrease with treatment time for each construct ($P < 0.01$; Fig. 1A and B). Initiating the MTT assay after three doubling times resulted in approximately 5% to 10% reduced viability relative to performing the assay after only one doubling time (Supplementary Fig. S5; one doubling time of PSMA-positive HUVEC was 36 hours).

Both types of targeted vesicles (white and grey bars in Fig. 1A and B) resulted in significantly greater kill ($P \leq 0.002$) of PSMA-positive HUVEC compared with vesicles containing no targeting group (white bars with tilted pattern) at 6 hours of incubation (Fig. 1C and D), for both static and flow conditions. The observed cell kill mediated by both types of targeted vesicles should not be attributed to leaked radioactivity (^{225}Ac-DOTA at 7.4 kBq/mL or 20% of 37 kBq/mL; at 6 hours; $P < 0.01$; Fig. 1C–F). Vesicles loaded with ^{225}Ac and labeled with a nonspecific antibody (white bars with horizontal pattern in Fig. 1C and D) or with a nonactive urea analog (gray bars with horizontal pattern in Fig. 1C and D) affected cell viability similarly to the ^{225}Ac-loaded vesicles containing no targeting group (white bars with tilted pattern).

Selectivity in affecting the viability of PSMA-positive HUVEC (Fig. 1A and B) relative to normal endothelium (PSMA-negative HUVEC; Fig. 1E and F) was indicated by the corresponding different cell viabilities ($P \leq 0.01$) at 6 hours of incubation for all radiolabeled targeted constructs, and at 10 hours of incubation for the radiolabeled antibody (Supplementary Table S3), both at the static and flow conditions.

On PSMA-negative HUVEC in static conditions, after one hour of incubation, Ab-targeted vesicles were more lethal than urea-targeted vesicles ($P = 0.007$). This finding cannot be supported by different radioactivity uptake by cells (Supplementary Table S2).

Interestingly, Fig. 2 (and Supplementary Fig. S6), which depicts the viability of cells (shown in Fig. 1) versus the corresponding uptake of radioactivity by cells (shown in Supplementary Table S2 as a function of time) for each of the constructs that were evaluated, shows that any level of associated radioactivity per cell resulted in greater killing efficacy when delivered by PSMA-targeting vesicles instead of the radiolabeled PSMA-targeting antibody. The presence of flow (Supplementary Fig. S7) did not affect efficacy.

Intracellular localization of constructs

PSMA-positive HUVEC incubated with PSMA-targeting antibody-labeled (red) and urea-labeled (purple) vesicles (Fig. 3A, first and second plots, respectively) exhibited punctate fluorescence within the cytoplasm and in the case of the urea-targeted vesicles, a pronounced perinuclear localization. The PSMA-targeting antibody (Fig. 3A, third panel, green) localized mainly in the region closer to the plasma membrane far from the nuclear envelop. Quantitative processing of images of all constructs (Fig. 3B), in the absence and presence of inhibitors, support these observations. Chlorpromazine, an inhibitor of clathrin-mediated endocytosis, did not affect the cell uptake (Fig. 3A, thin continuous lines) and the intracellular spatial distributions (Fig. 3B) of any construct. Genistein, an inhibitor of caveolae-mediated endocytosis, decreased the cell uptake of both types of targeted vesicles and of the antibody (Fig. 3A, dashed lines).

Presaturation of cells with the free PSMA antibody or the free lysine glutamate urea agent (Fig. 3C) significantly decreased the association of all constructs with cells demonstrating PSMA-specific receptor-mediated uptake.

Discussion

The major finding of this study is that radionuclide carriers (and in particular targeted lipid vesicles) that promote localization of ^{225}Ac close to the cell nucleus, further enhance the already high killing efficacy of the delivered activity of α-particle emitters compared with radionuclide carriers that localize close to the cell's plasma membrane (such as radiolabeled antibodies). Nuclear localization has been extensively explored for very short range emitters (such as of Auger electrons; ref. 5), but not for α-particle emitters probably with the exception in the context of boron neutron capture therapy (18) and one study on using a modular transporter of astatine-211 (19). We utilized lipid vesicles loaded with ^{225}Ac and labeled with a urea-based low-molecular-weight agent (11) and an antibody (20), both targeting the PSMA on human endothelial cells. Both types of vesicles improve the killing efficacy of delivered activity per cell by almost 3-fold relative to the killing efficacy of the same levels of activity when delivered by the

Figure 3.

A, intracellular spatial distribution (fused fluorescence and bright field images) and flow-cytometric shifts in the absence and presence of endocytosis inhibitors: first panel, Ab-targeted vesicles (red); second panel, urea-targeted vesicles (purple); third panel, fluorescently labeled antibody (green), in PSMA$^+$ HUVEC. Cell nuclei are stained in blue. Scale bar, 40 μm. B, corresponding quantitative intracellular distributions of Ab-targeted vesicles (red symbols), urea-based targeted vesicles (purple symbols), and the antibody (green symbols) in above incubating conditions. *n* indicates total number of analyzed cells. Error bars, SD of the means of analyzed cells. C, cell uptake (fused fluorescence and bright field images) and flow-cytometric shifts in the absence and presence of presaturation of cells with the free PSMA antibody or the free lysine glutamate urea agent at 1,000× excess relative to cell receptors.

Published OnlineFirst November 19, 2015; DOI: 10.1158/1535-7163.MCT-15-0207

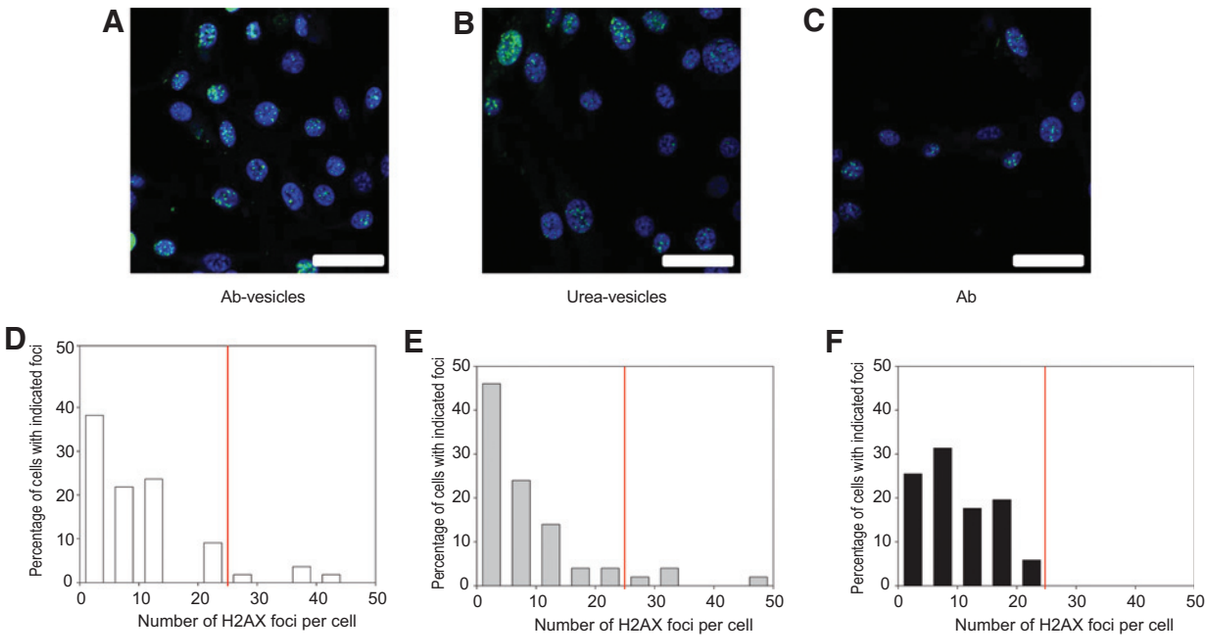

Figure 4.
Characteristic images obtained by immunofluorescent staining of γ-H2AX foci (green) in cell nuclei (blue), and distribution of the number of foci per cell nucleus upon exposure to the Ab-targeted vesicles (A), urea-targeted vesicles (B), and the radiolabeled Ab (C). Corresponding distributions of γ-H2AX foci per cell for Ab-targeted vesicles (white bars; D), urea-based targeted vesicles (gray bars; E), and the antibody (black bars; F) were obtained by counting at least 50 cells per case. The red line serves as a threshold to indicate the maximum limit of foci mediated by the radiolabeled antibody. Scale bar, 40 μm.

PSMA-targeting antibody (Fig. 2). The increase in killing efficacy, which is also accompanied by increased levels of dsDNAs (beyond the arbitrary threshold shown by the red line, Fig. 4; ref. 21), strongly correlates with intracellular patterns of vesicles exhibiting localization close to the cell nucleus, unlike the antibody which preferentially localizes near the plasma membrane during the period of observation (Fig. 3B). Other nanoparticles, not necessarily lipid vesicles, may result in similar perinuclear trafficking (22).

The observed spatial intracellular distributions of vesicles are expected to result in an increase of the effective solid angle of the (at least first) emitted α-particle (from the carrier-associated parent nuclide) with respect to the nucleus increasing, therefore, the probability of its trajectory crossing the nucleus. An approximate dosimetric analysis using the MIRDcell.v2.0 software (23) supports the above claims (Supplementary Table S4 for ^{225}Ac without daughters and Supplementary Table S5 for ^{225}Ac including radioactive daughters).

The choice of targeting ligand (in the sense of its role on altering the spatiotemporal intracellular distributions of the delivered nanoparticle) may affect the efficacy of nanoparticles as is suggested by a previous study on vesicles labeled with the PSMA targeting antibody J591 or the A10 aptamer (12) which demonstrated that only vesicles targeted with the J591 antibody perform similarly well as the radiolabeled antibody when compared in terms of radioactivity delivered per cell.

In the present studies, although the extent of endocytosis of both types of targeted vesicles and of the antibody is significantly decreased by the same inhibitor of caveolae-mediated endocytosis, their intracellular spatial distributions are dramatically different (Fig. 3B) suggesting the existence of potentially additional factors that govern the internalization mechanism(s) (22).

To enable further development of targeted vesicles as carriers of ^{225}Ac against easily accessibly cells (e.g., neovasculature) with relatively low copies of targeted receptors, at least two aspects of their design should be improved: the apparent K_D and the loading ratio of emitter to carrier. We have shown that the latter can in principle be improved by introducing greater radioactivity levels during loading which is equal to or greater than 47% of introduced radioactivity (for radioactivity levels up to at least 7.4 MBq). Decreasing the apparent K_D of targeted vesicles may be enabled by potentially optimizing the conjugation density of targeting ligands on vesicles (24) or the size of nanoparticles (25).

In summary, nanoconjugation of PSMA-targeting ligands using lipid vesicles loaded with ^{225}Ac improves the killing efficacy of delivered activity per cell by almost 3-fold relative to the killing efficacy of the same levels of activity per cell when delivered by the PSMA-targeting antibody. We attribute this finding to the perinuclear localization of the emitter when delivered by targeting vesicles that enhances the probability of emitted α-particles traversing through the cell nucleus.

Disclosure of Potential Conflicts of Interest

No potential conflicts of interest were disclosed.

Authors' Contributions

Conception and design: S. Sofou
Development of methodology: C. Zhu, A. Bandekar, F. Bruchertseifer
Acquisition of data (provided animals, acquired and managed patients, provided facilities, etc.): C. Zhu, A. Bandekar, M. Sempkowski

Analysis and interpretation of data (e.g., statistical analysis, biostatistics, computational analysis): C. Zhu, M.G. Pomper, F. Bruchertseifer, S. Sofou
Writing, review, and/or revision of the manuscript: C. Zhu, M.G. Pomper, F. Bruchertseifer, A. Morgenstern, S. Sofou
Administrative, technical, or material support (i.e., reporting or organizing data, constructing databases): M. Sempkowski, S.R. Banerjee, F. Bruchertseifer, A. Morgenstern, S. Sofou
Study supervision: S. Sofou
Other (provided those small-molecule PSMA inhibitors; material support): S. R. Banerjee

Acknowledgments

The authors thank Progenics Pharmaceuticals, Inc. for generously providing anti-PSMA antibody, in which it has a proprietary commercial interest. They also thank the High Resolution Microscopy Facility, Department of Biomedical Engineering, Rutgers University, and the Neuroscience Imaging Facility, W. M. Keck Center for Collaborative Neuroscience, Rutgers University.

Grant Support

This work was supported in part by the American Cancer Society Research Scholar Grant RSG-12-044-01, the National Science Foundation Grant DMR1207022 (to S. Sofou), NIH CA134675, CA184228, the A. David Mazzone Awards Program of the Prostate Cancer Foundation (to M.G. Pomper), and by the Charles and Johanna Busch Memorial Fund (to S. Sofou).

The costs of publication of this article were defrayed in part by the payment of page charges. This article must therefore be hereby marked *advertisement* in accordance with 18 U.S.C. Section 1734 solely to indicate this fact.

Received March 18, 2015; revised September 8, 2015; accepted October 16, 2015; published OnlineFirst November 19, 2015.

References

1. Thorpe PE. Vascular targeting agents as cancer therapeutics. Clin Cancer Res 2004;10:415–27.
2. Thorpe PE, Burrows FJ. Antibody-directed targeting of the vasculature of solid tumors. Breast Cancer Res Treat 1995;36:237–51.
3. Ruggiero A, Villa CH, Holland JP, Sprinkle SR, May C, Lewis JS, et al. Imaging and treating tumor vasculature with targeted radiolabeled carbon nanotubes. Int J Nanomedicine 2010;5:783–802.
4. Kennel SJ, Mirzadeh S, Eckelman WC, Waldmann TA, Garmestani K, Yordanov AT, et al. Vascular-targeted radioimmunotherapy with the alpha-particle emitter 211At. Radiat Res 2002;157:633–41.
5. Boswell CA, Brechbiel MW. Auger electrons: lethal, low energy, and coming soon to a tumor cell nucleus near you. J Nucl Med 2005;46:1946–7.
6. Dudley AC. Tumor endothelial cells. Cold Spring Harb Perspect Med 2012;2:a006536.
7. Chang SS, Reuter VE, Heston WDW, Bander NH, Grauer LS, Gaudin PB. Five different anti-prostate-specific membrane antigen (PSMA) antibodies confirm PSMA expression in tumor-associated neovasculature. Cancer Res 1999;59:3192–8.
8. Liu H, Moy P, Kim S, Xia Y, Rajasekaran A, Navarro V, et al. Monoclonal antibodies to the extracellular domain of prostate-specific membrane antigen also react with tumor vascular endothelium. Cancer Res 1997;57:3629–34.
9. Chandran SS, Banerjee SR, Mease RC, Pomper MG, Denmeade SR. Characterization of a targeted nanoparticle functionalized with a urea-based inhibitor of prostate-specific membrane antigen (PSMA). Cancer Biol Ther 2008;7:974–82.
10. Pommé S, Marouli M, Suliman G, Dikmen H, Van Ammel R, Jobbágy V, et al. Measurement of the ^{225}Ac half-life. Appl Radiat Isot 2012;70:2608–14.
11. Banerjee SR, Pullambhatla M, Byun Y, Nimmagadda S, Foss CA, Green G, et al. Sequential SPECT and optical imaging of experimental models of prostate cancer with a dual modality inhibitor of the prostate-specific membrane antigen. Angew Chem Int Ed Engl 2011;50:9167–70.
12. Bandekar A, Zhu C, Jindal R, Bruchertseifer F, Morgenstern A, Sofou S. Anti–prostate-specific membrane antigen liposomes loaded with 225Ac for potential targeted antivascular α-particle therapy of cancer. J Nucl Med 2014;55:107–14.
13. McDevitt MR, Ma D, Simon J, Frank RK, Kiefer GE, Scheinberg DA. Design and synthesis of actinium-225 radioimmunopharmaceuticals. Appl Radiat Isot 2002;57:841–7.
14. McDevitt MR, Barendswaard E, Ma D, Lai L, Curcio MJ, Sgouros G, et al. An alpha-particle emitting antibody ([213Bi]J591) for radioimmunotherapy of prostate cancer. Cancer Res 2000;60:6095–100.
15. Liu T, Jabbes J, Nedrow-Byers JR, Wu LY, Bryan JN, Berkman CE. Detection of prostate-specific membrane antigen on HUVECs in response to breast tumor-conditioned medium. Int J Oncol 2011;38:1349–55.
16. Chen Y, Pullambhatla M, Banerjee SR, Byun Y, Stathis M, Rojas C, et al. Synthesis and biological evaluation of low molecular weight fluorescent imaging agents for the prostate-specific membrane antigen. Bioconjug Chem 2012;23:2377–85.
17. Ballangrud AM, Yang W-H, Charlton DE, McDevitt MR, Hamacher KA, Panageas KS, et al. Response of LNCaP spheroids after treatment with an a-particle emitter (213Bi)-labeled anti-prostate-specific membrane antigen antibody (J591). Cancer Res 2001;61:2008–14.
18. Tung CJ, Liu CS, Wang JP, Chang SL. Calculations of cellular microdosimetry parameters for alpha particles and electrons. Appl Radiat Isot 2004;61:739–43.
19. Rosenkranz AA, Vaidyanathan G, Pozzi OR, Lunin VG, Zalutsky MR, Sobolev AS. Engineered modular recombinant transporters: application of new platform for targeted radiotherapeutic agents to α-particle emitting 211At. Int J Radiat Oncol Biol Phys 2008;72:193–200.
20. Schülke N, Varlamova OA, Donovan GP, Ma D, Gardner JP, Morrissey DM, et al. The homodimer of prostate-specific membrane antigen is a functional target for cancer therapy. Proc Natl Acad Sci 2003;100:12590–5.
21. Baidoo KE, Yong K, Brechbiel MW. Molecular pathways: targeted α-particle radiation therapy. Clin Cancer Res 2013;19:530–7.
22. Bhattacharyya S, Bhattacharya R, Curley S, McNiven MA, Mukherjee P. Nanoconjugation modulates the trafficking and mechanism of antibody induced receptor endocytosis. Proc Natl Acad Sci 2010;107:14541–6.
23. Vaziri B, Wu H, Dhawan AP, Du P, Howell RW, SNMMI MIRD Committee. MIRD pamphlet No. 25: MIRDcell V2.0 software tool for dosimetric analysis of biologic response of multicellular populations. J Nucl Med 2014;55:1557–64.
24. Elias DR, Poloukhtine A, Popik V, Tsourkas A. Effect of ligand density, receptor density, and nanoparticle size on cell targeting. Nanomedicine 2013;9:194–201.
25. Jiang W, KimBetty YS, Rutka JT, ChanWarren CW. Nanoparticle-mediated cellular response is size-dependent. Nat Nano 2008;3:145–50.

Published OnlineFirst November 19, 2015; DOI: 10.1158/1535-7163.MCT-15-0207

Molecular Cancer Therapeutics

Nanoconjugation of PSMA-Targeting Ligands Enhances Perinuclear Localization and Improves Efficacy of Delivered Alpha-Particle Emitters against Tumor Endothelial Analogues

Charles Zhu, Amey Bandekar, Michelle Sempkowski, et al.

Mol Cancer Ther 2016;15:106-113. Published OnlineFirst November 19, 2015.